SAND2018-13632R

The Relative Importance of Assumed Infrasound Source Mechanisms on the Linear Inversion of Infrasound Time Series at the Source Physics Experiment

Christian Poppeliers[1], Katherine Anderson Aur[1], and Leiph Preston[1]
1. Geophysics Department, Sandia National Laboratories, Albuquerque, NM

Abstract
We invert far field infrasound data for the equivalent seismo-acoustic time domain moment tensor to assess the relative importance of two assumed seismoacoustic source mechanisms. The infrasound data were produced by a four of the underground chemical explosions that were conducted during the Source Physics Experiment (SPE). For each SPE event that we invert, we produce three set of atmospheric Green's functions: an average model based on ten years of atmospheric data, as well as two extrema models designed to maximize the variability of atmospheric conditions for the given time-of-day and day-of-year for each SPE event. To parameterize the inversion, we assume that the source of infrasonic energy results from the linear combination of explosion-induced surface spall and linear seismic-to-elastic mode conversion at the Earth's free surface. We find that the inversion yields relatively repeatable results for the estimated spall source whereas the estimated isotropic explosion source is highly variable. This suggests that the majority of the observed acoustic energy is produced by the spall source and/or our modeling of the elastic energy propagation, and data are subsequent conversion to acoustic energy via linear elastic-to-acoustic coupling at the surface, is too simplistic.

Introduction
Fully and partially contained single-charge underground chemical explosions can be used as surrogates for underground nuclear explosions to study explosion source physics (e.g. Stump *et al.*, 1999; Arrowsmith *et al.*, 2010; Ford *et al.*, 2014; Gitterman *et al.*, 1998; Patton *et al.*, 2005). In addition to seismic energy, a significant amount of infrasonic energy can be generated, which can aid in the detection, discrimination, and forensic analysis of buried explosions (e.g. Che *et al.*, 2014). The two primary mechanisms of generating infrasonic acoustic energy include linear seismic-to-acoustic coupling at the Earth's surface and the near source effects of non-linear ground deformation (spall). In our case, we assume that spall takes the form of the ground physically upheaving, similar to the phenomenon modeled by the Rayleigh integral (e.g. Jones *et al*., 2015). A given explosion will excite these two mechanisms to differing degrees depending on the yield, scaled depth-of-burial, and geologic structure (Ford *et al*., 2014). Therefore, by inverting infrasonic data for the individual terms of an effective source model it is possible, in principle, to constrain the relative contribution of each mechanism for a given explosion event. In this report, we describe the results of inverting infrasonic data that was collected as part of the Source Physics Experiment (SPE) for the linear-equivalent time domain moment tensor (see Snelson *et al*., 2013, for details of SPE). In so doing, our primary goal is to determine the relative contribution of each presumed source mechanism to the observed infrasonic data.

Research Accomplished
Experimental Setup and Data
The SPE Phase 1 consisted of a series of six controlled and well-recorded chemical explosions at the Nevada National Security Site (NNSS), where factors such as depth-of-burial, explosive yield, and geology are controlled and/or reasonably known. We focus our work here on the infrasonic data that was produced from four of the SPE explosions. The data were collected on a

series of surface-mounted acoustic sensors (Figure 1) where the attempt was made to isolate the sensors from the explosion-generated seismic arrivals. All of the explosions occurred in the same borehole, located in granite bedrock, where the depth and yield of the explosive varied for each event (Table 1). Although six experiments were conducted over a span of approximately five years, we only analyze the data from four of the experiments due to acceptable signal-to-noise conditions. Furthermore, we only analyze the data collected at sensors located more than one kilometer from the source, thereby ensuring that seismic energy didn't superpose the acoustic energy. The acoustic sensors were arranged in arrays of four instruments and were distributed along two azimuthal directions: a single array of instruments was located approximately one kilometer due east from the explosion site and the other three arrays were located due south of the explosion site at approximate distances of one, two, and five kilometers.

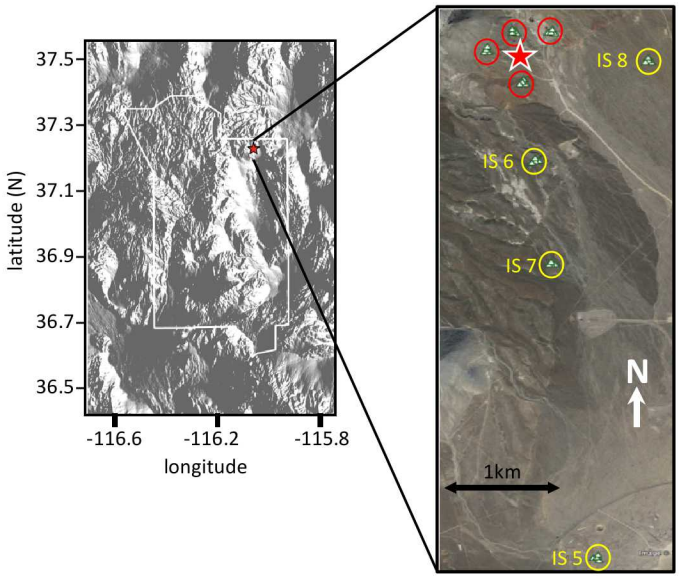

Figure 1. Location of SPE Phase 1. Left: Overview map showing the outline of the NNSS (in white), where the location of the experiment is shown by the red star. Right: Expanded view of the SPE Phase 1 area. The surface location of the explosions is shown by the red star and the infrasound stations are indicated by the yellow circles. The yellow numbers correspond to the arrays that we use in the analysis. Each array, approximately 50m in aperture, contained four infrasound stations in a triangular shape, with a single station in the center and three stations at the corners. The red circles indicate the locations of the infrasound arrays that are not analyzed in this paper due to the superposition of the seismic and infrasonic first arrivals.

Analysis

We use a frequency domain inversion technique (Stump and Johnson, 1977; Yang and Bonner, 2009) to invert for time dependent source moment tensors of the four explosions. The frequency domain approach allows us to resolve the relative contribution of the two presumed source mechanisms as well as their time evolution. The model assumes that the far-field data can be predicted by the linear superposition of the convolutions of an equivalent point seismo-acoustic sources with the Green's functions describing the atmosphere's impulse response (see Poppeliers *et al*., 2019 for details).

We explicitly assume that the source of the acoustic energy results from two mechanisms: 1) an explosion located underground and 2) explosion-generated spall, which is located at the Earth's

surface directly above the explosion. Note that the actual explosion occurs underground, resulting in non-linear deformation of the Earth in the immediate vicinity of the explosion. However, this region is small relative to the scale of the source-receiver distance, so we make the simplification that the explosion results in purely elastic seismic waves radiating from a point. The assumption is that the seismic energy from the explosion converts to acoustic energy at the Earth's surface via linear mode conversion. The second source term in our model attempts to simulate the spall of the Earth's surface directly above the explosion source. As with the explosion term, spall is highly non-linear, but over the scale of the source-receiver distance, the spall source is small enough to be approximated by a purely vertical, time-dependent force acting on the Earth's surface directly above the explosion source. For our model, we explicitly assume that the explosion source is a buried isotropic explosion and that the force term (simulating the spall) is a purely vertical, upwards directed point force acting on the Earth's surface.

Table 1: SPE Phase 1 data analyzed in this report. DOB is depth-of-burial and SDOB is scaled depth-of-burial

SPE Event	Date of experiment	Yield (tons)	DOB(m)	SDOB(m/kt$^{1/3}$)
SPE-1	3 May, 2011	1.0	45.7	457
SPE-3	24 July, 2012	0.9	47.2	488
SPE-5	26 April, 2016	5.04	76.5	446
SPE-6	12 October, 2016	2.2	31.4	241

In a previous report, we describe the construction of atmospheric models as well as the estimation of Green's functions which we will only summarize here in the interest of brevity. We used publically available, regional scaled atmospheric data to construct three atmospheric predictions for each SPE event. For each SPE event, we collect atmospheric data over a one-hour period that is centered at the day-of-year (DOY) and time-of-day (TOD) for the given SPE event and construct three models: the first model is constructed by averaging the ten snapshots of atmospheric data, and the second two models are constructed by selecting the years that represent the extrema conditions for the ten-year period. For each case, we extrapolate and interpolate the data onto a three-dimensional grid which we then use as input to a staggered grid finite difference routine that solves for the three-dimensional particle velocity and pressure for each model node. For each model, we construct two sets of Green's functions, one for each source term.

Results and Discussion

The inversion solves for the complex spectra of both source terms simultaneously, from which we obtained the time-domain source terms by applying the inverse Fourier transform (Figure 2). In general, we found that the inversion results contained small, high frequency components, likely a result of instability in the inversion. The most apparent result is that the estimated explosion source term is highly erratic for a given SPE event, depending on the atmospheric model. Additionally, the estimated explosion source

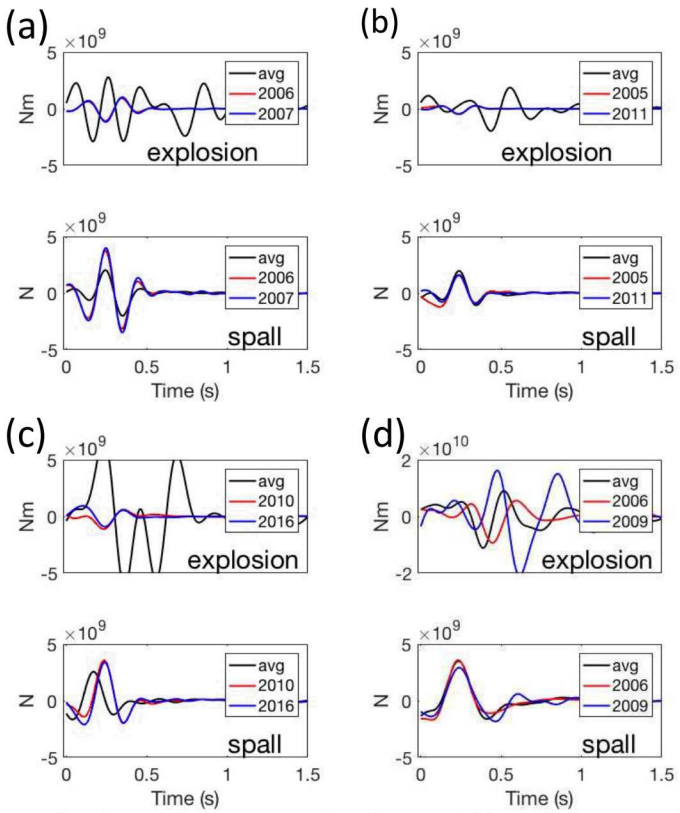

Figure 2: The inversion results, for each SPE event, band passed filtered to 1-5Hz: (a) SPE-2, (b) SPE-3, (c) SPE-5, (d) SPE-6. For each panel, we show the estimated time domain source terms for each presumed source mechanism: an isotropic explosion and the surface-located spall. The results obtained using the 10-year average atmospheric models are shown in black, and the results using the extrema models are shown in red and blue, according to the legend. Note that the results for the vertical force tensor term (i.e. spall) are quite stable and repeatable, whereas the results for the explosion term are not.

term is extremely variable from one SPE event to the next. Conversely, the estimated spall source term is remarkably similar for all four SPE events and from model to model. For SPE-1, the estimated explosion source term for the 10-year average atmospheric model is quite erratic and different from the estimated explosion source terms for the extrema atmospheric models. However, the explosion source terms estimated using the two extrema models are quite similar to each other. For the estimated spall terms, the wave forms and timing are similar, with the major difference being the smaller amplitude of the spall term estimated using the 10-year average model. The estimated explosion source terms for SPE-3 behave similarly to those of the SPE-2 event: the explosion source term for the 10-year average model is significantly different than those estimated using the extrema atmospheric models. Also, the explosion source terms for both of the extrema models are virtually identical. The estimated spall terms are remarkably similar for all three atmospheric models for SPE-3. The estimated explosion source terms for SPE-4 behave similarly to those of the SPE-2 and SPE-3 events: the explosion source term for the 10-year average model is significantly different, and higher amplitude, than those estimated using the extrema atmospheric models. The spall terms estimated using the extrema atmospheric models are virtually identical. The spall term estimated using the 10-year average model has a similar waveform as those estimated using the extrema models, but is advanced in time. It is unclear why this estimated spall term is advanced in time, as the data and Green's functions were

time-aligned prior to inversion. For SPE-4P, the estimated explosion terms are different for all three atmospheric models, showing no obvious similarities from one model to the next. However, the estimated spall terms are similar for all three models. For SPE 2, 3, and 5, the estimated explosion terms are similar for the extrema models whereas the explosion term estimated using the 10-year average model is the outlier. The relative amplitudes of the estimated spall terms don't appear to scale to the scaled depth-of-burial. If they did, we would expect the amplitude of these terms would all be roughly similar for SPE 2, 3, and 5 whereas the amplitude of the estimated spall term for SPE 6 would be roughly twice that of the other three. Finally, for all the events, regardless of the model, the explosion-only model fits the worst, the spall-only model fits good, but the explosion-plus-spall fits the best (Table 2). Thus, even though the explosion-only term doesn't appear to be able to fit the data very well, the explosion source term appears to be influencing the data to a small degree.

Table 2: The data misfit for three scenarios, for each SPE event and atmospheric model.

SPE event	atmos. model	expl. only	spall only	expl + spall
SPE-2	10-year	0.3480	0.1469	0.1140
	2006	0.9635	0.5678	0.1743
	2007	0.9654	0.6075	0.1684
SPE-3	10-year	0.8279	0.3451	0.2984
	2005	0.9673	0.5695	0.3138
	2011	0.9671	0.5339	0.2869
SPE-5	10-year	0.9029	0.6774	0.6083
	2010	0.9799	.06045	0.5082
	2016	0.9810	0.6117	0.5165
SPE-6	10-year	0.4851	0.3487	0.3147
	2006	0.6235	0.3421	0.2970
	2009	0.4169	0.3378	0.2927

In general, the inversion results fit the data extremely well. To illustrate this, for each SPE event we convolved the estimated source terms with the corresponding Green's functions, and summed the resulting time series. These time series are referred to as the predicted data, and is color in red in Figure 3.

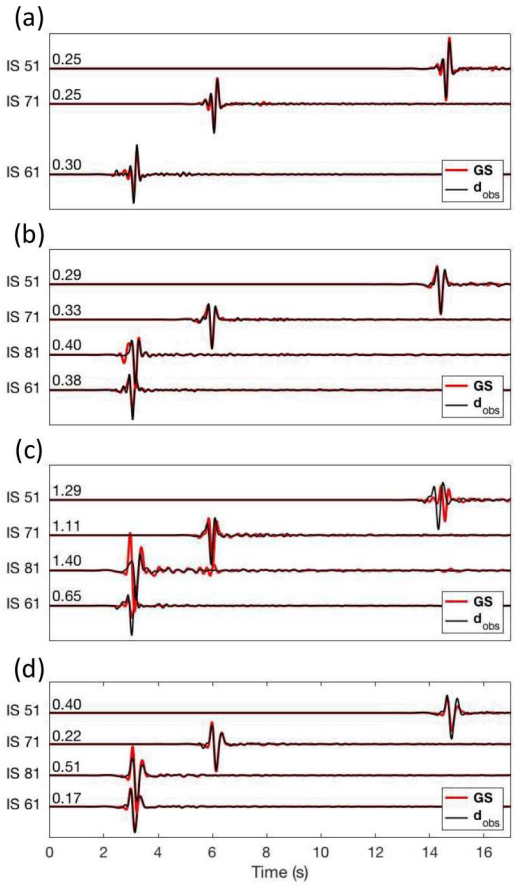

Figure 3: Comparison between the observed data (black) and the predicted data computed by convolving the estimated time domain moment tensor terms with the Green's functions estimated using the 10-year average atmospheric models (red). (a) SPE-2, (b) SPE-3, (c) SPE-5, and (d) SPE-6. The data misfit between the observed and synthetic data are marked above the traces. Note that for SPE-2 the data for station IS81 was not available. For this figure, the amplitudes of are trace normalized to the maximum amplitude of the observed data for each time series shown.

In Figure 3 we show the predicted data plotted on top of the observed data, bandpass filtered to 1-6 Hz. To assess the data misfit, we compute the residual and show this value on Figure 3 immediately above each predicted acoustogram. Because of space limitations, we only show one time series for each acoustic array and only for the 10-year average model. However, these results are typical, with the average data residual for all the data and all the models equal to 0.3244. The data misfit for SPE-5 was the worst, which we attribute to this event having the largest explosive yield. In this case the linear assumptions made in our inversion were violated to the greatest degree compared to the three other SPE events.

Based on our results, it appears that the estimated spall source term is relatively stable when using the different atmospheric models, suggesting that we can obtain robust estimates of the spall source term using only historical atmospheric data to predict the state of the atmosphere. However, our results show that the estimated explosion term to be highly sensitive to the predicted atmospheric model, which we interpret as follows: 1) the estimated explosion term

does not contribute significantly to the data and is thus not required to fit the data in the inversion, and 2) the poorly resolved explosion source term may be due to our forward model not simulating the effects of the buried explosion accurately.

Recall our assumption of two sources of infrasonic energy: the buried explosion and the surface spall. Our results show that for each SPE event, the estimated spall term is highly repeatable whereas the estimated explosion term is not. If both of the actual source terms were equal contributors to the data, we'd expect to see that both of the estimated source terms to be equally affected by the differences in the Green's functions, which is not the case. We interpret this as being the result of two reasons. First, the largest contributor to the infrasonic signal is the non-linear upheaval of the ground (spall), producing a momentary overpressure in the atmosphere. Although the spall is confined to a relatively small area of the ground surface (radius of 10s of meters) directly above the explosion, it has a vertical displacement amplitude of several centimeters. This is in contrast to the linear coupling of seismic energy into infrasonic energy, which occurs over a much larger area but with displacement amplitudes that are several orders of magnitudes lower than those associated with the spall. In this scenario, the relative contribution of the spall source term dominates the data. This explanation of the infrasonic signal generation is supported by the similarity of infrasonic data from SPE-2 and SPE-3 to synthetic infrasound data modeled by the Rayleigh integral (Jones *et al*., 2015; Whitaker, R., 2007, 2008, 2009). In these simulations, it was found that the data could be accurately explained by a single spall term, with no need for a contribution from a buried explosion term. Our results here appear to corroborate this, and lead us to conclude that the spall source term is the primary phenomenon responsible for the generation of the infrasonic signals observed at the SPE.

If the data contains very little actual contribution from the explosion source term, then the explosion source term may occupy the null space of the inversion: the estimated explosion source terms are virtually uninformed by the data, meaning that they can vary greatly without any significant obligation to fitting the data. The large degree of variation in the estimated explosion source term is likely due to noise in the data or errors in the estimated explosion Green's functions, which would have a relatively greater impact on this model parameter (Stump and Johnson, 1977). To test this assertion, we invert the data for three different scenarios, corresponding to three different assumed source mechanisms. Specifically, using the Green's functions for the 10-year average atmospheric model, we parameterize the inversion using only the spall term, only the explosion term, and then both of the source terms. We then invert the data for all four SPE events, and compute the average data misfit (Figure 4, Table 2). In all cases, when the data are inverted using only an explosion source term the average misfit is higher, with a greater degree of variability, than when we invert the data using a spall Green's function. Specifically, inverting the data for only the explosion term results in predicted data with underestimated amplitudes (Figure 4, Panels B and C), non-physical precursor arrivals (Figure 4, Panels A, B and D), and timing errors (Figure 4, Panel C). We interpret that these features in the predicted data are not due to the physics of this source term, but rather instabilities in the actual inversion that is likely due to either the explosion source term not contributing significantly to the data or the inaccuracy of our forward model. This result corroborates earlier works (e.g. Jones et al., 2015; Whittaker, 2007, 2008, 2009) which claimed that the dominant source of infrasound signal at SPE 2 and 3 is from surface spall rather than the linear elastic-to-acoustic coupling at the Earth's surface.

The second contributing factor to the instability of the estimated explosion source term may be that our forward model does not adequately simulate the seismic energy generated from the buried source. Specifically, the seismic wave field generated from a buried explosion is fully elastic, and will generate significant Rayleigh waves. In addition to the direct conversion of P-wave energy to acoustic energy, the propagation of surface waves will also generate an infrasonic signal (Artru *et al*., 2004; Mutschlecner and Whitaker, 2005). However, our method of modeling the acoustic Green's functions does not simulate elastic or Rayleigh waves. Rather, it treats the Earth as a fluid with a sound speed of 500 m/s, which precludes simulation of linear S-to-acoustic and Rayleigh-to-acoustic coupling. We view this as major limitation of this work, which we will address in a future work where we couple the elastic region of the model to an acoustic model. This combined model can then be used to more accurately estimate the acoustic Green's function resulting from the buried explosion source.

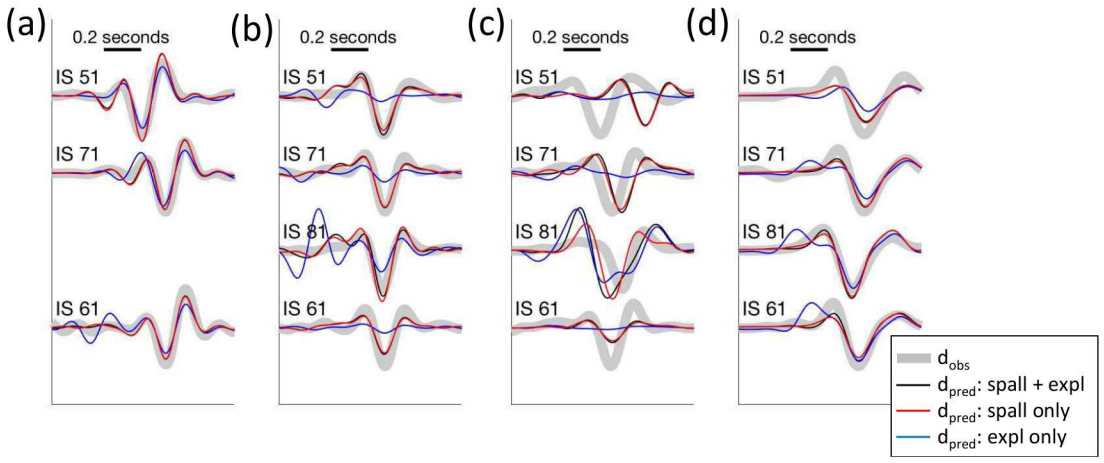

Figure 4: Data misfits for different source models. We show the observed data (black) for the first station from each array, for all four SPE events that we analyze. The panels are arranged from left to right as (a) SPE-2, (b) SPE-3, (c) SPE-5, and (d) SPE-6. Note that we window the data about the approximate first acoustic arrival for clarity. We show the predicted data where the assumed model is parameterized by both a spall and explosion term (black), a spall term only (red), and an explosion term only (blue). The observed data are shown as the heavy gray curve. To compute the synthetic data, we convolve the estimated source term with the relevant Green's function (see text). Note the high degree of data misfit when the inversion is parameterized by only an explosion term. For each event/station, the data are trace normalized to the maximum amplitude of the observed data.

Conclusions

The results of the inversion showed that the estimated spall term is relatively stable and repeatable for all of the SPE data that we invert, regardless of the atmospheric model that we used. Conversely, the estimated explosion term is highly variable in all cases. When we invert the data for only a spall term, the results are also stable and repeatable with a very low degree of data misfit.

The stability/repeatability of the estimated spall term, in the form of an effective vertical force, suggests that the spall term is the primary influence on the data. Conversely, the explosion term is not a significant contributor to the observed infrasonic data and/or our model of the elastic-to-

acoustic linear mode conversions is too simplistic to accurately estimate the explosion source. Regardless, for this work, the data can be explained and fit well using only a spall source term (simulated as a vertical point force) in the source model.

Given our limited suite of atmospheric predictions, it appears that using publicly available, regional scaled weather data may be adequate to estimate the equivalent source terms by inverting the infrasound resulting from buried explosions, when the source model is surface spall. We attribute variations in the estimated spall source terms as being due to variations in the predicted atmospheric models, but these atmospheric variations don't appear to degrade the spall source estimates to the point of un-reliability. The variations in the explosion source terms are likely due to either the explosion term not influencing the data and/or our overly simplistic modeling of this term.

The model of atmospheric sound propagation needs to accurately simulate both elastic and acoustic wave fields and any elastic-to-acoustic coupling that would result from a buried explosion. To test whether the buried, isotropic explosion term is an actual contributor to the observed data, it is necessary to more accurately simulate the elastic-to-acoustic mode conversions. Specifically, our inversion simulated the Earth as a fluid with a high acoustic velocity, which precluded the simulation of actual elastic energy. Seismic wave fields are known to contribute to infrasonic energy via linear body wave to acoustic and Rayleigh to acoustic mode conversions. We will address these phenomena in future work.

Acknowledgements
Sandia National Laboratories is a multimission laboratory managed and operated by National Technology & Engineering Solutions of Sandia, LLC, a wholly owned subsidiary of Honeywell International Inc., for the U.S. Department of Energy's National Nuclear Security Administration under contract DE-NA0003525. This paper describes objective technical results and analysis. Any subjective views or opinions that might be expressed in the paper do not necessarily represent the views of the U.S. Department of Energy or the United States Government.

References
Arrowsmith, S.J., J.B. Johnson, D.P. Drob, and M.A.H. Hedlin (2010), The seismoacoustic wavefield: A new paradigm in studying geophysical phenomena, *Rev. Geophys.* **48**, doi:10.1029/2010RG000335.

Artru, J., T. Farges, and P. Lognonne (2004). Acoustic waves generated from seismic surface waves: propagation properties determined from Doppler sounding observations and normal-mode modeling, *Geophys. J. Int.* **158**, 1067-1077.

Che, I-Y, J. Park, I Kim, T. S. Kim, H-I Lee (2014). Infrasound signals from the underground nuclear explosions of North-Korea, *Geophys. J. Int.* **198**(1), 495-505. doi: 10.1093/gji/ggu150.

Ford, S.R., A.J. Rodgers, H. Xu, D.C. Templeton, P. Harben, W. Foxall, and R.E. Reinke (2014), Partitioning of Seismoacoustic Energy and Estimation of Yield and Height-of-Burst/Depth-of-Burial for Near-Surface Explosions, *Bull. Seis. Soc. Am.* **104**(2), 608-623, doi:10.1785/0120130130.

Gitterman, Y., Z. Ben-Avraham, and A. Ginzburg (1998). Spectral analysis of underwater explosions in the Dead Sea, *Geophys. J. Int.* **134**, 460-472.

Jones, K.R., R.W. Whitaker, S.J. Arrowsmith (2015). Modelling infrasound signal generation from two underground explosions at the Source Physics Experiment using the Rayleigh integral, *Geophys. J. Int.* **200**, 779-790. doi: 10.1093/gji/ggu443.

Mutschlecner, J.P., and R.W. Whitaker (2005). Infrasound from Earthquakes, *J. of Geophys. Res.* **110**, doi: 10.1029/204JD005067.

Patton, H.J., J.L. Bonner, and N. Gupta (2005). Rg excitation by underground explosions: insights from source modeling the 1997 Kazakhstan depth-of-burial experiment, *Geophys. J. Int.* **163**, 1006-1024.

Poppeliers, C., K.A. Aur, L. Preston (2010) The relative importance of assumed infrasound source terms and effects of atmospheric models on the linear inversion of infrasound time series at the Source Physics Experiment, *Bull. Seis. Soc. Am.* **in publication**

Snelson, C.M., R.E. Abbot, S.T. Broome, R.J. Mellors, H.J. Patton, A. J. Sussman, M.J Townsend, W.R. Walter (2013). Chemical Explosion Experiments to Improve Nuclear Test Monitoring, *EOS, Trans. Am. Geophys. Un.*, **94**(27), 237-239.

Stump, B.W and L.R. Johnson (1977). The determination of source properties by the linear inversion of seismograms, *Bull. Seis. Soc. Am.* **67**, 1489-1502.

Whitaker, R., 2007. Infrasound signals as basis for event discriminants, in *Proceedings of the 29th Monitoring Research Review: Ground-Based Nuclear Explosion Monitoring Technologies*, LA-UR-07-5613, Vol. 1, pp. 905-913, Available at: http://www.osti.gov.bridge/product.biblio.jsp?osti$_$id=1027449.

Whitaker, R., 2008. Infrasound signals as basis for event discriminants, in *Proceedings of the 30th Monitoring Research Review: Ground-Based Nuclear Explosion Monitoring Technologies*, LA-UR-08-05261, Vol. 1, pp. 912-920, Available at: http://www.osti.gov.bridge/product.biblio.jsp?osti$_$id=960561.

Whitaker, R., 2009. Infrasound signals as basis for event discriminants, in *Proceedings of the 30th Monitoring Research Review: Ground-Based Nuclear Explosion Monitoring Technologies*, LA-UR-09-05276, Vol. 1, pp. 750-758, Available at: http://www.osti.gov.bridge/product.biblio.jsp?osti$_$id=992203.

Yang, X. and J.L. Bonner (2009). Characteristics of Chemical Explosive Sources from Time-Dependent Moment Tensors, *Bull. Seis. Soc. Am.* **99**(1), 36-51, doi: 10.1785/0120080243.